# Optimization of damping function parameters for -D3 and -D4 dispersion models for Hartree-Fock based symmetry-adapted perturbation theory

Austin M. Wallace<sup>1</sup> and C. David Sherrill<sup>2, a)</sup>

(Dated: 14 January 2025)

Symmetry-adapted perturbation theory (SAPT) directly computes an intermolecular interaction energy in terms of electrostatics, exchange-repulsion, induction/polarization, and London dispersion components. In SAPT based on Hartree-Fock ("SAPTO") or based on density functional theory, the most time-consuming step is the computation of the dispersion terms. Previous work has explored the replacement of these expensive dispersion terms with simple damped asymptotic models. We recently examined [J. Chem. Phys. 154, 234107 (2021)] the accuracy of SAPT0 when replacing its dispersion term with Grimme's popular -D3 correction, reducing the computational cost scaling from  $\mathcal{O}(N^5)$  to  $\mathcal{O}(N^3)$ . That work optimized damping function parameters for SAPT0-D3/jun-cc-pVDZ using estimates of the coupled-cluster complete basis set limit [CCSD(T)/CBS] on a 8299 dimer dataset. Here we explore the accuracy of SAPT0-D3 with additional basis sets, along with an analogous model using -D4. Damping parameters are rather insensitive to basis set, and the resulting SAPT0-D models are more accurate on average for total interaction energies than SAPT0. Our results are surprising in several respects: (1) improvement of -D4 over -D3 is negligible for these systems, even charged systems where -D4 should in principle be more accurate; (2) addition of Axilrod-Teller-Muto (ATM) terms for three-body dispersion does not improve error statistics for this test set; (3) SAPT0-D is even more accurate on average for total interaction energies than the much more computationally costly density functional theory based SAPT [SAPT(DFT)] in an aug-cc-pVDZ basis. However, SAPT0 and SAPT0-D3/D4 interaction energies benefit from significant error cancellation between exchange and dispersion terms.

# I. INTRODUCTION

The interaction energy ( $\Delta E_{\rm int}$ ) between two monomers measures the strength of their attraction or repulsion at a fixed dimer geometry. It may be computed in a "supermolecular" approach as in Eq. 1, where I and J designate monomers and IJ symbolizes the dimer.

$$\Delta E_{\text{int}} = E_{IJ} - E_I - E_J. \tag{1}$$

Alternatively,  $\Delta E_{\rm int}$  can be directly computed using symmetry-adapted perturbation theory (SAPT), which provides not only the total quantum  $\Delta E_{\rm int}$ , but also its physical components: electrostatics ( $E_{\rm elst}$ ), exchange ( $E_{\rm exch}$ ), induction/polarization ( $E_{\rm ind}$ ), and dispersion ( $E_{\rm disp}$ ) energies.<sup>1–5</sup> Unfortunately, even the least computationally expensive variant of SAPT, sometimes called SAPT0, scales as  $\mathcal{O}(N^5)$ , limiting the applicability to a few hundred atoms at most. This level of SAPT computes the intermolecular interactions to second-order based on a Hartree-Fock (HF) description of the monomers (i.e., intramolecular electron correlation is neglected):

$$\begin{split} \Delta E_{\rm int} \; \approx \; E_{\rm SAPT0} &= E_{\rm elst}^{(10)} + E_{\rm exch}^{(10)} + E_{\rm ind,resp}^{(20)} \\ &+ E_{\rm exch-ind,resp}^{(20)} + \delta_{\rm HF}^{(2)} + E_{\rm disp}^{(20)} + E_{\rm exch-disp}^{(20)} (2) \end{split}$$

The superscripts  $[E^{(vw)}]$  designate v as the intermolecular interaction perturbation order and w as the perturbation order for intramolecular electron correlation. To simplify the analysis, our group counts the exchangeinduction cross term as part of the induction energy  $E_{\rm ind}$ , and the exchange-dispersion cross term as part of the dispersion energy  $E_{\rm disp}$ . Also, the  $\delta_{\rm HF}^{(2)}$  term accounts for the difference in energy between the HF interaction energy and the sum of the SAPT0 electrostatics, exchange, and induction components, which are all captured at the Hartree-Fock level; this largely corrects for higher-order induction contributions beyond second order. Therefore, the  $\delta_{\rm HF}^{(2)}$  is pulled into  $E_{\rm ind}$  term when describing the energy in terms of four components. The correction  $\delta_{\rm HF}$ itself is infinite-order (as it incorporates a Hartree-Fock interaction energy that is fully self-consistent), but the (2) superscript is a reminder that the correction is meant to be applied to SAPT energetics that are at most 2ndorder in v. We may group the SAPT0 contributions as shown in Eq. 3-4, and Eq. 5 emphasizes that  $E_{\text{SAPT0}}$  is equivalent to the HF interaction energy plus a dispersion correction.

$$E_{\text{SAPT0}} = [E_{\text{elst}}^{(10)}] + [E_{\text{exch}}^{(10)}] + [E_{\text{ind,resp}}^{(20)} + E_{\text{exch-ind,resp}}^{(20)} + \delta_{\text{HF}}^{(2)}] + [E_{\text{disp}}^{(20)} + E_{\text{exch-disp}}^{(20)}],$$
(3)

$$= (E_{\text{elst}} + E_{\text{exch}} + E_{\text{ind}}) + E_{\text{disp}}, \tag{4}$$

$$\equiv E_{\rm int}^{\rm HF} + E_{\rm disp}. \tag{5}$$

Dispersion is the most computationally expensive com-

<sup>&</sup>lt;sup>1)</sup> Center for Computational Molecular Science and Technology and School of Chemistry and Biochemistry, Georgia Institute of Technology, Atlanta, GA 30332-0400

<sup>&</sup>lt;sup>2)</sup> Center for Computational Molecular Science and Technology, School of Chemistry and Biochemistry, and School of Computational Science and Engineering, Georgia Institute of Technology, Atlanta, GA 30332-0400

a) Electronic mail: sherrill@gatech.edu

ponent in a SAPT0 calculation. Excluding this term reduces the scaling of SAPT0 to  $\mathcal{O}(N^3)$  in our density-fitted atomic orbital based implementation, <sup>6,7</sup> which makes computations on large systems more feasible. Fortunately, the two-body (2B) dispersion may be computed rather accurately in the asymptotic limit through a simple series of the form

$$E_{\text{disp,2B}} = -\sum_{A < B} \sum_{n=6.8,10...} \frac{C_n^{AB}}{R_{AB}^{(n)}},\tag{6}$$

where the summation can be over unique pairs of molecules (using molecular coefficients  $C_n^{AB}$ ) or unique pairs of atoms (using atomic coefficients  $C_n^{AB}$ ). Here we consider a sum over pairs of atoms. Such an expression, usually truncated at n = 6, is commonly used to capture dispersion interactions between non-bonded atoms in the popular force fields used in molecular dynamics. Such expressions can also provide a reliable model of dispersion interactions at intermediate and short ranges, although in the latter case, it is important to multiply them by suitable damping functions to avoid divergence of the dispersion energy as  $R_{AB}$  becomes small. These kinds of functional forms have a long history of use in quantum chemistry, dating back to "Hartree-Fock plus dispersion" (HFD) models, <sup>8-10</sup> and then the very popular density functional theory plus dispersion (DFT-D)  $models^{11-15}$  and newer semi-empirical models like HF- $3c^{16}$  and PBEh- $3c.^{17}$ 

Such dispersion corrections have also been applied in the context of SAPT, which might be broadly called "SAPT-D" models. In a test for He<sub>2</sub>, Misquitta and Szalewicz<sup>18</sup> found that a damped asymptotic expansion for dispersion worked well in conjunction with the SAPT(KS) method, which is analogous to SAPT0 except that Kohn-Sham orbitals are used, and the exchangecorrelation functional must be made to have the proper asymptotic limit.<sup>19</sup> SAPT(KS) seemed to work well for first-order energies but not second-order energies (induction and dispersion), and this was attributed to the KS virtual orbital energies, which appear in the sum overstates expressions for those two energy components, being underestimated; 19 this was the motivation for Misquitta and Szalewicz to examine damped multipolar expansions of the dispersion as a replacement for the sumover-states expression for this term. 18

In 2010, Szalewicz and co-workers<sup>20</sup> revived and improved the HFD method by adding first-order electron correlation corrections to the electrostatics and exchange terms as computed by DFT-based SAPT, also called SAPT(DFT)<sup>21</sup> or SAPT-DFT,<sup>22</sup> which is an improvement over the original SAPT(KS) scheme. When using damped asymptotic dispersion terms (including  $C_6^{AB}/R_{AB}^6$  and  $C_8^{AB}/R_{AB}^8$  terms), they denote their scheme as HFD<sub>as</sub>c<sup>(1)</sup>. In 2011, Hesselmann<sup>23</sup> used a set of 22 van der Waals dimers, each at five geometries, to test the accuracy of DFT-D and a SAPT(DFT) approach in which the dispersion terms were replaced by

a damped asymptotic correction. For the SAPT-D approach, a single term in the expansion was used, scaled by a factor of 0.67, with an interatomic distance dependence of  $R_{AB}^{-5.67}$ . A customized damping function, based on an error function, was developed specifically for this SAPT-D approach. Although it suffices to damp the dispersion correction to zero at short distances in DFT-D (because some short- and intermediate-range dispersiontype interactions are thought to be captured by the supermolecular DFT computation), the correction needs to remain finite in SAPT-D-type approaches because the entirety of the dispersion interaction is being modeled by the -D correction.  $^{23}$   $C_6$  dispersion coefficients and atomic van der Waals radii (used in the damping function) taken from Grimme's DFT-D2 approach. 13 The result was roughly similar accuracy for SAPT-D and the DFT-D approach tested (B97-D2 with Becke's original parameterization of the B97 functional).

In 2012, Lao and Herbert<sup>24</sup> adopted this -D correction to replace the expensive sum-over-states dispersion term in their explicit polarization plus symmetry-adapted perturbation theory approach, yielding a method referred to as XSAPT(KS)+D or XPS(KS)+D.<sup>24</sup> This approach gave promising results for the S22A<sup>25</sup> and S66<sup>26</sup> test sets, along with several other individual test cases. In 2013 these authors updated the form of the -D correction  $^{27,28}\,$ to that used by Szalewicz and co-workers<sup>20</sup> in their  $HFD_{as}c^{(1)}$  approach. In 2015, to address occasional overestimation of dispersion in  $\pi$ -stacked systems, they introduced their third-generation dispersion correction,<sup>29</sup> later dubbed aiD3, for use with XSAPT(KS). This dispersion correction used the same damped  $C_6$  and  $C_8$ form as their previous iteration (with Tang-Toennies damping),  $^{30,31}$  but now the damping parameters and atomic  $C_6^A$  and  $C_8^A$  coefficients were all fit to high-level SAPT dispersion values (atom-pair coefficients are obtained using the common combining rule  $C_n^{AB} =$  $\sqrt{C_n^A C_n^B}$ ). Except of the special case of hydrogen, where its bonding partner was taken into account, the fitted atomic coefficients  $C_n^A$  were dependent only on the atomic number, and not the chemical environment. In 2019, Herbert and co-workers<sup>32</sup> examined an alternative approach of using the many-body dispersion (MBD) method of Tkatchenko and co-workers<sup>33,34</sup> rather than aiD3 in conjunction with their XSAPT(KS) method. MBD includes all higher-order dispersion effects, but only the dipole-dipole type response terms; thus, it was supplemented by short-range damped  $C_8$  terms to represent dipole-quadrupole response terms.<sup>32</sup> The XSAPT+MBD method, as well as XSAPT+aiD3 plus an Axilrod-Teller-Muto (ATM)<sup>35,36</sup> treatment of three-body dispersion, showed significant improvement over XSAPT+aiD3 for the L7 test set<sup>37,38</sup> of large van der Waals dimers.

In 2017, Sedlak and Řezáč<sup>39</sup> updated Hesselmann's SAPT -D correction for SAPT(DFT) based on Grimme's third-generation (-D3) dispersion correction. <sup>14</sup> The form of this correction (and the newer -D4 correction) $^{40-42}$  is

given by

$$E_{2B}^{D3/D4} = -\sum_{A < B} \sum_{n=6.8} s_n \frac{C_{(n)}^{AB}}{R_{AB}^{(n)}} f_{damp}^{(n)}(R_{AB}), \quad (7)$$

which now includes  $C_8$  terms.  $s_6$  is fixed to 1 to provide physically correct long-range behavior, but  $s_8$  is allowed to be a fitted parameter. Sedlak and Řezáč obtained parameters suitable to use in conjunction with SAPT(DFT) by fitting to SAPT(DFT) dispersion energies of 66 van der Waals dimers, each in 8 different geometries, from the S66x8 dataset. <sup>26,43</sup> They considered a generalized form of Hesselmann's damping function, as well as the Tang-Toennies damping function, and found that the latter worked better on average.

Use of the newer Grimme-type dispersion corrections has a number of advantages. The model includes both  $C_6$  and  $C_8$  contributions, it uses the physically-correct  $R^{-6}$  functional form at long distance, it damps contributions at short range, parameters are already available for most elements, and the dispersion coefficients are adjusted based on the local chemical environment (as described fully below). In addition, the corrections are already available as an independent software component that is readily interfaced to other software.

For these reasons, in 2021 our group optimized the global damping parameters in -D3 for use with Hartree-Fock-based SAPT, i.e. SAPT0, which is equivalent for interaction energies to HF-D3 (the SAPT approach of course retains the energy component decomposition, which can provide significant chemical insight).<sup>4</sup> The D3 approach already provides damping parameters suitable for use with Hartree-Fock, but our study refitted them to a much larger set of 8299 van der Waals dimers. We chose to fit SAPT0-D3 to benchmark interaction energies computed by coupled-cluster through perturbative triples, CCSD(T), 46 in the complete-basis-set (CBS) limit. CCSD(T)/CBS reference energies have been employed in some of the previously mentioned studies on fitting -D corrections, while other studies have chosen to fit high-level SAPT dispersion energies, so that the correction does not absorb contributions not related to dispersion. We prefer CCSD(T)/CBS interaction energies, as this choice minimizes the total error in the interaction energies. Moreover, because we are using a functional form developed to model dispersion, which has the correct asymptotic form, it seems to us that the resulting fitted function is prevented from behaving in a way that is significantly unphysical, although the dispersion energies will admittedly be adjusted to be larger or smaller as needed to provide better error cancellation for the overall total interaction energy.

The damping of short-range interactions in -D3 serves a role analogous to the exchange-dispersion cross term in SAPT0. Thus, we can replace the entirety of the SAPT0  $E_{\rm disp}$  with the -D3 model of the dispersion interaction energy,  $E_{\rm int}^{\rm D3}$ , to yield

$$E_{\text{SAPT0-D3}} = E_{\text{int}}^{\text{HF}} + E_{\text{int}}^{\text{D3}}.$$
 (8)

Details on how we compute  $E_{\rm int}^{\rm D3}$  are provided in the Theoretical Methods section below.

Our previous study examined several damping functions for use in SAPT0-D3: Becke-Johnson (BJ),<sup>47</sup> zero-damping/Chai-Head-Gordon (CHG),<sup>48</sup> and modified CHG (mCHG),<sup>49</sup> and the BJ damping function yielded the lowest errors (this is perhaps not surprising, as the CHG damping function damps dispersion contributions too quickly at short range<sup>50</sup> is thus not appropriate for use in SAPT applications, where unlike in DFT-D applications, the short-range dispersion contributions need to be captured by the -D correction). The resulting approach was referred to as SAPT0-D3M(BJ) the M in D3M refers to modification of the damping parameters from the original recommended HF parameters (determined for a smaller training set). At the time, we focused exclusively on the jun-cc-pVDZ basis aug-cc-pVDZ basis $^{51}$  that deletes diffuse functions on H atoms and diffuse d functions on heavy atoms), <sup>52,53</sup> due to favorable error cancellation between this basis and the SAPT0 method.<sup>54</sup> SAPT0-D3M(BJ) in this modest basis set resulted in a mean absolute error (MAE) of 0.488 kcal  $\mathrm{mol^{-1}}$ , root-mean-square-error (RMSE) of 0.833 kcal  $\mathrm{mol^{-1}}$  and a maximum absolute error (MaxAE) of  $14.070 \text{ kcal mol}^{-1}$  on the 8299-dimer dataset.<sup>50</sup>

More recently, Villot and Lao<sup>55</sup> produced a dataset of nearly 10,000 SAPT interaction energies at the reliable SAPT2+(3)(CCD)/aug-cc-pVTZ level, and used them to perform a similar reparameterization of the three global parameters in Grimme's -D3 model, for use in (X)SAPT models. They also performed a similar reparameterization of the MBD model, as supplemented by  $C_8$  terms. They then further improved the model by developing a machine-learning-based correction to address remaining discrepancies between the reparameterized D3/MBD model and the reference SAPT dispersion energies. For their test set, the D3-ML model exhibits mean absolute errors for dispersion energies of only 0.14 kcal mol<sup>-1</sup> vs high-level SAPT.

Although these recent works have focused on Grimme's third-generation -D3 model, the fourth-generation model -D4, has been reported as far back as 2017.<sup>40–42</sup> This begs the question of whether significant improvements could be had by replacing -D3 with -D4 in schemes such as those just described. Our current interest is in its use together with SAPTO, i.e.,

$$E_{\text{SAPT0-D4}} = E_{\text{int}}^{\text{HF}} + E_{\text{int}}^{\text{D4}}.$$
 (9)

Presumably, -D4 should improve overall error statistics vs -D3, and in particular one would expect it to improve errors for systems with large partial atomic charges due to updates in -D4 allowing it to take atomic charges into account when computing  $C_6$  values.<sup>41</sup>

Grimme recommends  $^{40}$  adding three-body dispersion corrections to -D4 by default, using an Axilrod-Teller-Muto (ATM) formula  $^{35,36}$  for atom triplets.

$$E^{ABC} = \frac{C_9^{ABC} (3\cos\theta_{BAC}\theta_{ACB}\theta_{CBA} + 1)}{(R_{AB}R_{AC}R_{BC})^3}, \quad (10)$$

where A, B, and C to refer to atoms. Thus, it is also of interest to see how error statistics behave when this term is included or not.

In the present paper, we revisit our 2021 study<sup>50</sup> to see how much improvement is afforded by using -D4 instead of -D3 to model dispersion in SAPT0, again using our large 8299-dimer test set. We also remedy a deficiency of the previous study, namely, its focus on only one basis set (jun-cc-pVDZ). Here we consider SAPT0-D3 and SAPT0-D4 with seven basis sets, and we examine the sensitivity of the of the optimized damping parameters to the basis set chosen. We also examine how the error statistics change whether or not the ATM model of three-body dispersion is used. Finally, we compare the resulting models to the popular SAPT(DFT) approach<sup>21,22</sup> to address their relative accuracy.

# II. THEORETICAL METHODS

Before describing the test sets and optimization procedures, we first discuss the details of how we compute the -D3/-D4 contributions to the interaction energy,  $E_{\rm int}^{\rm D3/D4}$ , and then we review the -D3/-D4 approaches and discuss the improvements made in the -D4 model.

# A. Details on Computing $E_{\mathrm{int}}^{\mathrm{D3/D4}}$

In the -D3 and -D4 models, the  $C_6$  and consequently  $C_8$  coefficients are partially dependent on the atomic environment, and so they change slightly when computed in the dimer versus when they are computed in a monomer, hence necessitating computation via a "supermolecular" approach:

$$E_{\rm int}^{{\rm D3/D4}} = E_{IJ}^{{\rm D3/D4}} - (E_I^{{\rm D3/D4}} + E_J^{{\rm D3/D4}}). \eqno(11)$$

As a practical matter, when interfacing to external software to compute the -D correction, such as Grimme's DFTD3 or DFTD4 programs, <sup>44,45</sup> the supermolecular computation according to Eq. 11 is very straightforward.

After choosing this supermolecular approach in our previous work,<sup>50</sup> we came across a cautionary note in the previously-mentioned work of Sedlak and Řezáč.<sup>39</sup> Those authors also preferred a supermolecular approach. due to the simplicity of implementing it. However, they commented that "The resulting difference in the  $C_6$  coefficient" (from the monomer to the dimer geometry) "is negligible, but it propagates into the  $C_8$  coefficient, which is derived from it ... Because of the steep slope of the  $C_8/r^8$  term at short distances, even this small difference may lead to a large change in the interaction dispersion energy. This effect is hidden by the damping in DFT-D3 but becomes large when no or less aggressive damping is used, such as in this case. We have fixed this issue by using integer valence numbers that are the same in the dimer and in the monomers. This approximation is

perfectly valid in the context of DFT-SAPT calculations where only the intermolecular dispersion between well-defined molecular species is calculated (i.e., no covalent bonds are being broken). In such cases, rounding the valence numbers to integers does not affect the accuracy of the  $C_6$  coefficients but removes the unwanted artifacts."

Based on these comments, we performed some tests in which we alternatively defined the dispersion interaction energy  $E_{\rm int}^{{\rm D3/D4}}$  in an intermolecular sense, i.e., we restricted the sum over atom pairs to those in which one atom comes from monomer I, and the other comes from monomer J (in the limit that changes in the chemical environment upon dimerization are small enough to not change the  $C_6$  coefficients, this becomes an equivalent definition, because intramolecular dispersion contributions will cancel). This alternative definition should be another way to circumvent the numerical issues mentioned by Sedlak and Řezáč. Upon reoptimization of global damping parameters with this alternative definition, our error statistics were very slightly improved (Supplemental Material Figure S4). However, the improvement did not seem large enough to warrant a change in procedure. Additionally, we examined the challenging potential curves of doubly hydrogen-bonded dimers in the HBC6 test set, <sup>56,57</sup> to make sure the supermolecular approach yielded smooth interaction energy curves. The result, shown in Supplemental Material Figure S4, is indeed smooth (the intermolecular definition is also smooth and gives very similar although not identical results). Thus, we cannot rule out that there are any problematic aspects to the supermolecular definition, but we did not find any obvious evidence of them. Another reason to prefer the supermolecular definition, besides its ease of implementation, is that switching to an intermolecular definition would mean that SAPT0-D would no longer be equivalent to HF-D for interaction energies; however, the solution of Sedlak and Řezáč sidesteps this problem and would maintain their equivalence (if it were also applied to HF-D).

# B. Differences Between -D3 and -D4

The -D3 and -D4 dispersion corrections are similar, with small differences for constructing the  $C_6^{AB}$  values that are required by Eq. 7. Both corrections simply require a molecular geometry as input to compute  $C_6^{AB}$  by interpolation of tabulated data. The -D3/-D4 models utilize tables of reference molecular imaginary frequency-dependent dipole polarizabilities,  $\alpha(i\omega)$ , that are used to estimate corresponding reference atomic values  $\alpha^A(i\omega)$ . Those values, in turn, are used to estimate reference coefficients,  $C_{6,\text{ref}}^{AB}$ , between every pair of atoms A and B in the molecule using a modified Casimir-Polder formula: A

$$C_{6,\text{ref}}^{AB} = \frac{3}{\pi} \int_0^\infty \alpha^{A,\text{ref}}(i\omega) \alpha^{B,\text{ref}}(i\omega) d\omega.$$
 (12)

Finally (as discussed in more detail below), these coefficients  $C_{6,\text{ref}}^{AB}$  are used to compute the final  $C_{6}^{AB}$  through a scaling procedure that accounts for the local chemical environment around atoms A and B.

Due to atom-in-molecule dynamic polarizabilities being impossible to compute directly, the -D3/-D4 approaches have a scheme for estimating them using reference molecules  $A_m X_n$ . A reference atomic polarizability  $\alpha^{A,\text{ref}}$  for atom A within the reference molecule can be acquired by subtracting a hydrogen or halogen contribution from the reference system and dividing by m to get back to a single atom's polarizability,  $^{40}$ 

$$\alpha^{A,\text{ref}}(i\omega) = \frac{1}{m} \zeta(z^{A,\text{ref}}, z^{A}) [\alpha^{A_{m}X_{n}}(i\omega) - \frac{n}{2} \alpha^{X_{2}}(i\omega) \zeta(z^{X_{A,\text{ref}}}, z^{X_{2}})]. \quad (13)$$

For -D4,  $\zeta$  rescales atomic polarizabilities based on effective nuclear charges ( $z^A = Z^A + q^A$ , where  $q^A$  are atomic partial charges calculated by default by the electronegativity equilibration technique<sup>41</sup>) and chemical hardness, <sup>59</sup>  $\gamma^A$ . Note that  $z^A$  is the atomic charge of atom A in the target molecule of interest, whereas the other z values pertain to the reference molecules in the internal database. No such scaling is applied in -D3. <sup>40,41</sup> Thus,

$$\zeta(z^{A,\text{ref}}, z^{A}) = \begin{cases} 1 & , -D3\\ exp[3\{1 - exp[\gamma^{A}(1 - \frac{z^{A,\text{ref}}}{z^{A}})]\}] & , -D4. \end{cases}$$
(14)

This is one of the major differences in  $C_6$  construction between -D3 and -D4.

The final  $C_6^{AB}$  values needed by Eq. 7 can be computed from the reference values  $C_{6,\text{ref}}^{AB}$  by scaling them to account for the local electronic environment around each atom; this is represented by a coordination number (CN), which is allowed to be a fractional number. -D3 computes the CN for atom A by summing covalently bonded close contacts through using scaled covalent radii ( $R_{A,\text{cov}}$  and  $R_{A,\text{cov}}$ ) in the following equation:

$$CN^{A} = \sum_{B \neq A}^{N_{atoms}} \frac{1}{1 + e^{-k_{1}(k_{2}(R_{A,cov} + R_{B,cov})/R_{AB}^{-1})}}, \quad (15)$$

Here,  $k_1 = 16$  and  $k_2 = \frac{4}{3}$ . CN's are then used to scale the  $C_{6,\text{ref}}$ 's to acquire the final  $C_6$ 's to use in Eq. 7, according to

$$C_6^{AB}(CN^A, CN^B) = \frac{\sum_{i}^{N_A} \sum_{i}^{N_B} C_{6, \text{ref}}^{AB} L_{ij}}{\sum_{i}^{N_A} \sum_{i}^{N_B} L_{ij}}.$$
 (16)

with  $N_A$  the number of reference molecules for atom A (likewise for B), and  $L_{ij}$  is given by  $^{14}$ 

$$L_{ij} = e^{-k_3[(CN^A - CN_i^A)^2 + (CN^B - CN_j^B)^2]}.$$
 (17)

We note that the -D4 correction can dynamically use multiple exponentials in  $L_{ij}$  to help distinguish between reference systems with similar coordination numbers, as explained in Ref. 41.

The -D4 correction computes the CN's using electronegativities (EN) to discern between covalent and ionic bonding, thus requiring additional reference systems:  $^{40}$ 

$$CN^{A} = \sum_{B \neq A}^{N_{\text{atoms}}} \frac{(k_{1}exp[|EN_{A} - EN_{B}| + k_{2}]^{2})}{2k_{3}} \times [1 + erf(-k_{0}(\frac{R_{AB} - R_{AB}^{cov}}{R_{AB}^{cov}}))], \qquad (18)$$

Additionally, CN equations in -D4 use an error function instead of an exponential. The resulting two-body  $C_6$ 's have improved, shifting their mean relative deviation from 4.7% (-D3) to 3.7% (-D4) with respect to experimental dipole-dipole dispersion coefficients.<sup>40</sup>

 $C_8$  coefficients are estimated from  $C_6$  coefficients in both -D3 and -D4:<sup>31,60,61</sup>

$$C_8^{AB} = -3C_6^{AB} \sqrt{Q^A Q^B}, (19)$$

where  $Q^A$  and  $Q^B$  depend on multipole-type expectation values  $(\langle r^4 \rangle$  and  $\langle r^2 \rangle)$  derived from atomic densities.<sup>42</sup>

$$Q^A = s_{42}\sqrt{Z^A} \frac{\langle r^4 \rangle^A}{\langle r^2 \rangle^A},\tag{20}$$

and  $s_{42}$  is a constant fit to ensure that  $C_8^{AA}$  values for He, Ne and Ar are reasonable for -D3; in -D4,  $s_{42}$  is set to 1.<sup>14</sup>

In -D3, the Becke-Johnson (BJ) damping function<sup>47,50,62,63</sup> became the preferred one to damp the two-body dispersion terms from Eq. 7,<sup>64</sup> and this is the only one implemented in the Grimme's DFTD4 program directly.

$$f_{damp_{BJ}}^{(n)}(R_{AB}) = \frac{R_{AB}^{(n)}}{R_{AB}^{(n)} + (a_1 R_0^{AB} + a_2)^{(n)}}.$$
 (21)

The BJ damping function depends on  $R_{AB}$  as the distance between atom A and atom B and  $R_{0,BJ}^{AB} = \sqrt{C_8^{AB}/C_6^{AB}}$ . The damping parameters  $a_1$ ,  $a_2$ , and  $s_8$  in -D3 and -D4 are optimized and tabulated for each density functional and wavefunction method independently.

A damped ATM equation is used to account for three-body dispersion effects in -D3/-D4 according to

$$E^{ABC} = \sum_{A < B < C} f_{damp}^{(9)}(\vec{r}_{ABC}) C_9^{ABC} \times \frac{3\cos\theta_{BAC}\theta_{ACB}\theta_{CBA} + 1}{(R_{AB}R_{AC}R_{BC})^3}.$$
 (22)

The dispersion coefficient can be approximated as  $C_9^{ABC} \approx -\sqrt{C_6^{AB}C_6^{AC}C_6^{BC}}$ , 14 using the already acquired pairwise  $C_6$ 's. ATM is typically disabled when

using -D3. Meanwhile, -D4 enables ATM by default using a damping function inspired by the CHG form for 2B dispersion:<sup>41,48</sup>

$$f_{\text{damp,3B-CHG}}^{(9)}(R_{ABC}) = \frac{1}{1 + 6(R_{ABC})^{-16}},$$
 (23)

with  $R_{ABC}$  defined as

$$R_{ABC} = \left(\frac{R_{AB}R_{AC}R_{BC}}{R_{0BJ}^{AB}R_{0BJ}^{AC}R_{0BJ}^{BC}}\right)^{1/3}.$$
 (24)

Although the two-body  $C_6$ 's are charged scaled (Eq. 14) in -D4, the  $C_6$ 's used to estimate  $C_9$ 's for ATM are not adjusted similarly.<sup>42</sup>

#### C. Datasets and Computations

Previous work by Caldeweyher et al. 41 selected intermolecular interaction energies to fit their -D4 BJ and ATM damping function parameters. Their dataset consists of \$66x8, 65 \$22x5, 66 and NCIBLIND10, 67 providing 718 benchmark datapoints for fitting damping parameters to intermolecular interaction energies. 41 Because \$APT0-D4\$ total interaction energies are equivalent to HF-D4 total interaction energies (\$APT0-D4\$ providing the additional benefit of the energy components), we can use the HF-D4 damping parameters of Caldeweyher et al. (see Table I) as an initial guess for \$APT0-D4\$ damping parameter optimization for our larger training set.

The present work uses a dataset that is larger by an order of magnitude, assembled from previous work,  $^{50}$  to optimize damping function parameters. The larger dataset should help ensure that the damping parameters are generally applicable across a wide range of non-covalent interactions. The dataset for all optimizations herein is composed of the ACHC,  $^{68}$  C<sub>2</sub>H<sub>4</sub> · NH<sub>4</sub>,  $^{56}$  CO<sub>2</sub> · NPAC,  $^{69}$  CO<sub>2</sub> · PAH,  $^{69}$  CO<sub>2</sub> · NT,  $^{69}$  CH<sub>4</sub> · NT,  $^{69}$  HBC6,  $^{56,57}$  NBC10x,  $^{49,56,70}$  S22x7,  $^{49,66,71}$  S66x10,  $^{26,49}$  X31x10,  $^{72}$  BBI,  $^{73}$  SSI,  $^{73}$  and Water2510  $^{74-76}$  test sets, amounting to a total of 8299 dimers with reference data at the estimated complete-basis-set (CBS) limit for coupled-cluster through perturbative triples, CCSD(T).  $^{46}$  These estimates were obtained using focal-point computations  $^{77,78}$  at the MP2/CBS +  $\Delta$ CCSD(T)/aug-cc-pVDZ level or better, where  $\Delta$ CCSD(T) denotes the difference between MP2 and CCSD(T).

The component analysis is performed on a dataset that contains high-level SAPT energies computed in another work,  $^{79}$  using the aug-cc-pVDZ and aug-cc-pVTZ basis sets. This dataset consists of 4558 van der Waals dimers, pulling together geometries from the SSI,  $^{73}$  S66x8,  $^{26,49}$  HBC6,  $^{56,57}$  NBC10ext,  $^{49,56,70}$  X31x10,  $^{50,72}$  and Ion43 $^{50,79,80}$  test sets. Then, a smaller subset with high-level SAPT up to the aug-cc-pVQZ basis contains 358 dimers obtained by combining HBC6, Ion38, and a subset of S66x8.

To compute SAPT0-D4 interaction energies, the SAPT0 interaction energies for the 8299 dimers are computed with seven basis sets (cc-pVDZ, jun-cc-pVDZ, aug-cc-pVDZ, cc-pVTZ, may-cc-pVTZ, jun-cc-pVTZ, and aug-cc-pVTZ) using the newly developed hrcl\_jobs python library<sup>81</sup> to execute Psi4 calculations<sup>82</sup> in a distributed parallel manner. Additionally, we also compare to results from density functional theory based SAPT, called SAPT(DFT) or DFT-SAPT, 21,22,83,84 using a recent implementation in Psi4.85 Due to quantitative errors and incorrect generalized gradient approximation exchange-correlation potential decay as exponential instead of 1/r, SAPT(DFT) utilizes the gradientregulation asymptotic correction (GRAC) scheme to improve accuracy. 86,87 This scheme requires the computation of an energy shift for the GRAC, which is the difference between the ionization potential and the Kohn-Sham highest occupied molecular orbital (HOMO) energy. The ionization potential for each monomer is estimated here by subtracting the energy of the cation form of the monomer from the neutral monomer. As is customary for SAPT(DFT), the PBE0 functional<sup>88,89</sup> was employed, and the aug-cc-pVDZ and aug-cc-pVTZ basis sets were used. For simplicity, in the following, the basis set names are abbreviated like aTZ for aug-cc-pVTZ, etc., where "a" is replaced with "j" or "m" for truncated jun-cc-pVXZ or may-cc-pVXZ basis sets, respectively. 53

Parameter optimizations are performed using scipy's optimize submodule.90 The Powell method is used because it is a gradient-free minimization algorithm.  $^{91,92}$ and we use the RMSE between SAPT0-D4 and CCSD(T)/CBS as the loss function (or error metric), consistent with the previous SAPT0-D3 study.<sup>50</sup> To accelerate optimization of damping function parameters, the  $C_6$ 's from DFT-D3 and DFT-D4 are stored for each dimer system to avoid re-computing these values for each set of new parameters during minimization. Furthermore, functions for computing the two-body and threebody dispersion terms are written in C++ and made accessible to scipy through pybind11.93 The code is accessible on GitHub and provides options to optimize parameters for two-body dispersion and three-body (ATM) dispersion with different ATM damping functions.<sup>94</sup> To ensure the code operates correctly, pytest tests<sup>95</sup> were written to match DFT-D4 output 2B and 3B dispersion energies.

or 9, with the  $E^{D3/D4}$  dispersion correction coming from

$$E^{\text{D3/D4}} = -\sum_{A < B} s_{6} f_{damp}^{(6)}(R_{AB}, \mathbf{a_{1}}, \mathbf{a_{2}}) \frac{C_{(6)}^{AB}}{R_{AB}^{(6)}} - \sum_{A < B} \mathbf{s_{8}} f_{damp}^{(8)}(R_{AB}, \mathbf{a_{1}}, \mathbf{a_{2}}) \frac{C_{(8)}^{AB}}{R_{AB}^{(8)}}, + \sum_{A < B < C} \mathbf{s_{9}} f_{damp}^{(9)}(R_{ABC}, \mathbf{a_{3}}, \mathbf{a_{4}}) C_{9}^{ABC} \times \frac{3\cos\theta_{BAC}\theta_{ACB}\theta_{CBA} + 1}{(R_{AB}R_{AC}R_{BC})^{3}},$$
(25)

where the damping function parameters that are optimized ( $\mathbf{s_8}$ ,  $\mathbf{s_9}$ ,  $\mathbf{a_1}$ ,  $\mathbf{a_2}$ ,  $\mathbf{a_3}$ , and  $\mathbf{a_4}$ ) are indicated in bold type. The two-body -D4 optimizations only vary  $\mathbf{s_8}$ ,  $\mathbf{a_1}$ , and  $\mathbf{a_2}$ , with  $\mathbf{s_9} = 0$ . For models including three-body ATM corrections, denoted -D4(ATM), we explored the possibility of independently varying the parameters in the ATM damping function,  $\mathbf{a_3}$  and  $\mathbf{a_4}$ . Some tests also allow  $\mathbf{s_9}$  to vary from the usual value of 1, but this did not appear to lead to any significant improvement and is not theoretically well justified. In the original HF-D4, the ATM damping terms  $\mathbf{a_3}$  and  $\mathbf{a_4}$  were set equal to the  $C_6$  damping terms  $\mathbf{a_1}$  and  $\mathbf{a_2}$ , respectively. 41

#### III. RESULTS AND DISCUSSION

#### A. Basis Set Effects

The present work optimizes parameters for SAPT0-D3 and SAPT0-D4 for different basis sets to see if parameters have a large basis set dependence. The optimized damping parameters for 2B SAPT0-D3 and 2B SAPT0-D4 are tabulated in Table I. Figure 1 displays errors for optimized SAPT0-D3 and conventional SAPT0, for several basis sets, versus CCSD(T)/CBS reference values.

One can quickly deduce that SAPT0 errors often get worse as the basis set becomes larger, especially with MaxAE. The SAPT0 MAE does improve by adding the jun and aug diffuse functions to cc-pVDZ, but the added diffuse functions for cc-pVTZ do not exhibit a similar benefit. In fact, the MAE values increase as more diffuse functions are added. Similarly, the error statistics also become worse when going from double- $\zeta$  to triple- $\zeta$ . In SAPT0, the dispersion term is an intermolecular analog of MP2, meaning that it can lead to substantial overbinding of polarizable systems, such as complexes with  $\pi-\pi$ -stacking in which the error amplifies with larger basis sets  $^{73,96-98}$ 

This failure of SAPT0 surprisingly can be cleaned up by the -D3 model, supporting the notion that the dispersion term is the cause of these errors worsening with larger basis sets. Comparing error statistics between SAPT0/aDZ versus SAPT0-D3/aDZ, the MAE decreases by approximately 0.15 kcal mol<sup>-1</sup> and MaxAE drops by

TABLE I. The SAPT0-D3 and SAPT0-D4 Becke-Johnson (BJ) damping parameters

Method	$s_8$	$a_1$	$\overline{a_2}$
$\overline{\text{HF-D3(BJ)/def2-QZVP}^a}$	0.917	0.339	2.883
$HF-D3/jun-cc-pVDZ^b$	0.713	0.080	3.628
$HF-D4/def2-QZVP^c$	1.617	0.450	3.357
SAPT0-D3/cc-pVDZ	0.768	0.097	3.643
SAPT0-D3/jun-cc-pVDZ	0.714	0.079	3.633
SAPT0-D3/aug-cc-pVDZ	0.738	0.095	3.637
SAPT0-D3/cc-pVTZ	0.786	0.114	3.653
SAPT0-D3/may-cc-pVTZ	0.764	0.107	3.645
SAPT0-D3/jun-cc-pVTZ	0.762	0.109	3.646
SAPT0-D3/aug-cc-pVTZ	0.763	0.111	3.648
SAPT0-D4/cc-pVDZ	0.820	0.628	1.440
SAPT0-D4/jun-cc-pVDZ	0.800	0.694	1.108
SAPT0-D4/aug-cc-pVDZ	0.831	0.706	1.124
SAPT0-D4/cc-pVTZ	0.868	0.717	1.145
SAPT0-D4/may-cc-pVTZ	0.859	0.716	1.132
SAPT0-D4/jun-cc-pVTZ	0.857	0.717	1.135
SAPT0-D4/aug-cc-pVTZ	0.856	0.718	1.137

<sup>a</sup> HF-D3(BJ) parameters from fitting to an intermolecular and intramolecular dataset. <sup>15</sup> <sup>b</sup> Two-body HF-D3 (equivalently SAPT0-D3) parameters from Schriber et al. <sup>50</sup> fit to interaction energies. <sup>c</sup> Caldeweyher et al. 's HF-D4(ATM) parameters fit to interaction energies. <sup>41</sup>

over 6 kcal mol<sup>-1</sup> for SAPT0-D3. The differences between SAPT0/aTZ and SAPT0-D3/aTZ error statistics are more stark, with the MAE dropping by about half (0.44 kcal mol<sup>-1</sup>) and a MaxAE reduction of nearly 20 kcal mol<sup>-1</sup>. SAPT0-D3 also tends to reduce variations between basis sets (because non-dispersion terms are captured at the Hartree-Fock level, and Hartree-Fock is not so sensitive to the basis set). Thus, the very slight further improvements in error statistics when going from SAPT0-D3/aDZ to SAPT0-D3/aTZ do not seem to warrant the increased computational costs for most applications.

The sensitivity of the damping function parameters to basis set for SAPT0-D3 is explored in Figure S1 of the Supplemental Material. The error statistic improvement in using fully optimized parameters versus keeping fixed aDZ parameters is negligible, even though the parameters themselves do change somewhat as can be seen in Table I.

Similarly to SAPT0-D3 parameterization, SAPT0-D4 damping function parameters are optimized separately for each basis set (Figure 2). The accuracy of SAPT0-D4 is improved by adding diffuse functions to both double- $\zeta$  and triple- $\zeta$  basis sets. Once again, there is not a significant improvement in MAE or RMSE upon going from aDZ to any augmented TZ basis set, although there is a reduction in the maximum error. Ultimately, the error statistics for SAPT0-D4 improve slightly over the SAPT0-D3 results across every basis set; however, practically speaking, these models have about the same level of accuracy. The most noticeable difference is a typical reduction in the maximum error of the test set by around

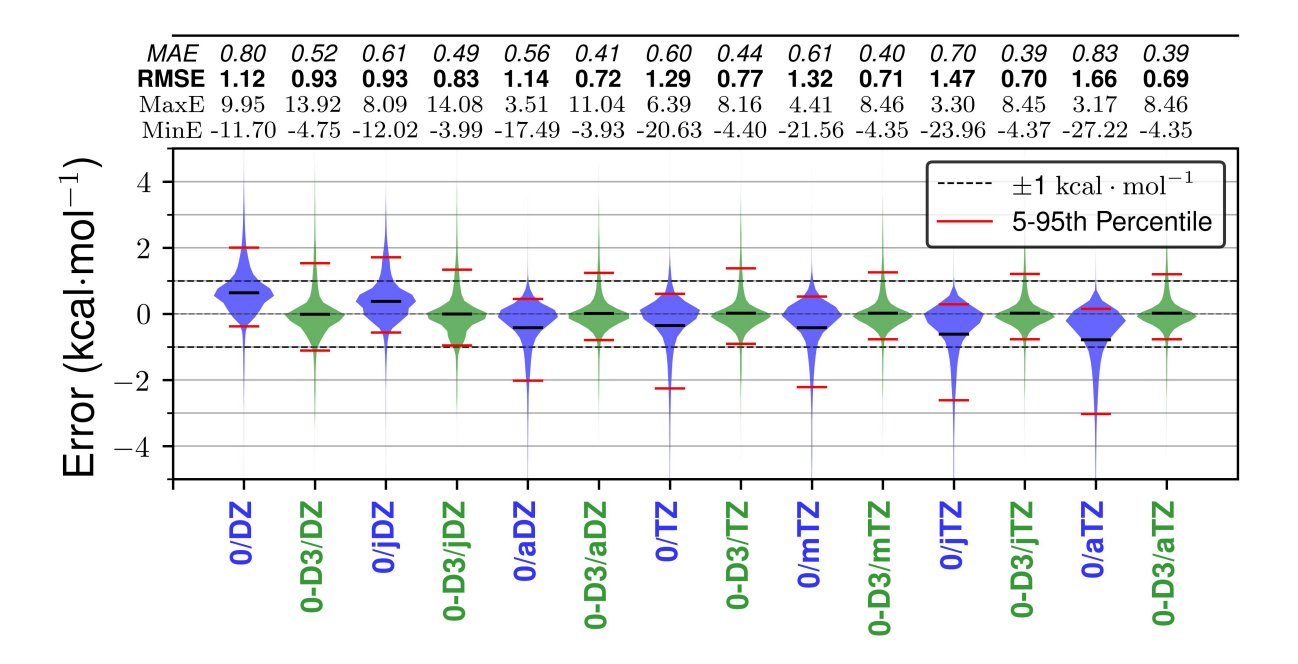


FIG. 1. Error of SAPT0 and SAPT0-D3 versus estimated CCSD(T)/CBS interaction energies for the 8299-dimer test set. SAPT0-D3 BJ damping parameters are optimized separately for each basis set. SAPT0 is labeled as "0" for simplifying the x-labels. The error statistics for each level of theory are tabulated above the violin plot.

# $1 \text{ kcal mol}^{-1}$ .

Just like in the SAPT0-D3 case, SAPT0-D4 parameters optimized at the SAPT0-D4/aug-cc-pVDZ level of theory yield very similar error statistics as the fully optimized parameters for each basis set (Figure S2). In general, the SAPT0-D4 damping parameters are quite consistent across basis sets, with somewhat larger differences for the cc-pVDZ basis set (Table I). As such, we recommend using the SAPT0-D3/aDZ and SAPT0-D4/aDZ parameters universally for other basis sets and not performing additional optimizations.

The marginal difference in error statistics between 2B SAPT0-D4 and 2B SAPT0-D3 was surprising to us; we expected the more advanced -D4 model to provide a noticeable improvement. However, it is also true that the -D4 model is largely similar to the -D3 model, with slightly improved accuracy for  $C_6$  coefficients, and one might have expected it to handle charged systems better due to its newly introduced charge scaling. Since the improvements of -D4 over -D3 should affect charged systems the most, we examine charged systems in more detail below.

Based on previous works favoring the TT damping function, the present work performed similar optimizations of damping function parameters and compared results with the BJ damping function (Supplemental Material Figure S3). The error statistics are slightly more favorable towards BJ for 2B dispersion across every basis set.

# B. ATM

Because the original -D4 model was designed to be used together with an ATM model of three-body dispersion, a proper investigation into SAPT0-D4 should also consider what happens when ATM terms are included, which we denote SAPT0-D4(ATM). Thus, additional optimizations were performed to obtain optimal damping parameters for this model (see Eq. 25). First, before moving on to parameter optimization, we consider what improvement the ATM terms might make when we utilize SAPT0-D4(ATM) with Grimme's original HF-D4(ATM) parameters. Figure 3 compares these results versus 2B SAPT0-D4 with our optimized damping parameters. For some system types like CO<sub>2</sub> with the partial nanotubes, nitrogren-doped polyheterocyclic aromatics (NPHAC's), or polycyclic aromatic hydrocarbons (PAH's), the addition of ATM does shift the error distribution in the correct direction, showing some merit for using ATM. Notably, these are among the largest systems in the present dataset, which would be in agreement with previous work suggesting that ATM contributions are more important for larger systems. 32,99 However, methane interacting with the partial nanotubes and PAH's does not show a clear benefit from using ATM. The Grimme parameters for the ATM term seem to fail for the close-range systems in S22x7 and S66x10, with large maximum errors. These results seem to imply that the parameters for the 3B-CHG damping function used in the ATM term require re-optimization on the larger dataset to account for these closer contact situations.

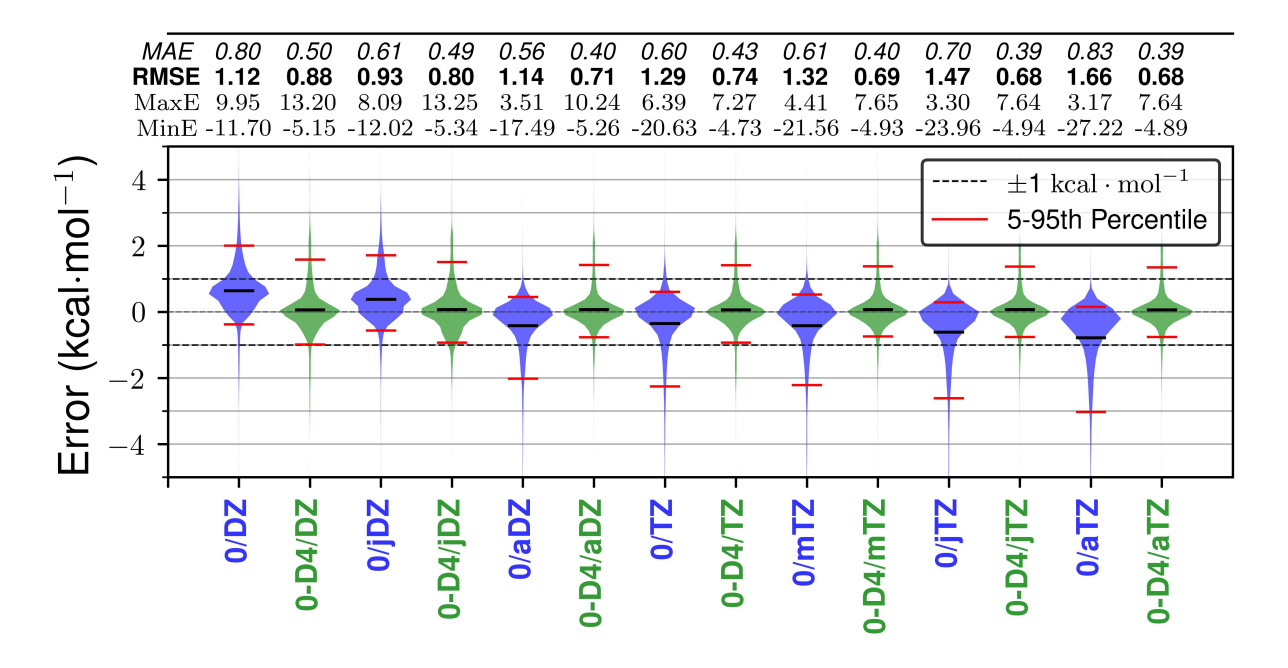


FIG. 2. Error of SAPT0 and SAPT0-D4 versus estimated CCSD(T)/CBS interaction energies for the 8299-dimer test set. SAPT0-D4 BJ damping parameters are optimized separately for each basis set. All -D4 corrections included only two-body terms. SAPT0 is labeled as "0" for simplifying the x-labels. The error statistics for each level of theory are tabulated above the violin plot. SAPT0-D4/aDZ has approximately the same **RMSE** and MAE as SAPT0-D4 using the augmented triple- $\zeta$  basis sets.

Several different schemes for optimizing the ATM damping function parameters were explored with the aug-cc-pVDZ basis set, because we anticipate that the damping parameters are probably insensitive to the basis set, by analogy to our findings to the 2B damping parameters as seen in Supplementary Material Figures S1 and S2. The first scheme was to use common damping parameters for both 2B and 3B terms, by optimizing  $a_1, a_2, \text{ and } s_8 \text{ (setting } a_1 = a_3 \text{ and } a_2 = a_4 \text{ from Eq.}$ 25). This approach is labeled SAPT0-D4(ATM) and actually yielded slightly worse results than the optimized 2B -D4, as can be seen in Figure 4. Next, a strategy we label SAPT0-D4(ATMu) optimizes separate damping terms for the 2B and 3B terms, effectively unrestricting the constraint of  $a_1 = a_3$  and  $a_2 = a_4$ . This approach allows optimization of  $s_8$ ,  $a_1$ ,  $a_2$ ,  $a_3$ , and  $a_4$  individually; however, the optimized values of the  $a_3$  and  $a_4$  terms make the denominator of the damping function to grow drastically larger than the numerator, effectively turning off the ATM portion. Thus, for these small dimers (with an average of 18 atoms, and a maximum of 42 atoms), the ATM terms do not appear to be helpful in improving agreement versus our benchmark CCSD(T)/CBS interaction energies. It would appear that the 2B -D4 terms can effectively capture the 3B terms implicitly, for these smaller systems at least. More improvement might be expected for larger systems. 32,99

# C. SAPT0-D4 versus SAPT(DFT)

Figure 4 also compares 2B SAPT0-D4 to results from the significantly more sophisticated (and computationally costly) SAPT(DFT) method. 85 SAPT0-D4/aDZ outperforms SAPT(DFT)/aDZ in terms of MAE and RMSE by 0.23 and 0.22 kcal  $\text{mol}^{-1}$ , respectively. This is remarkable given that SAPT0-D4 in our implementation is an  $\mathcal{O}(N^3)$  model, whereas depending on the implementation, SAPT(DFT) scales as  $\mathcal{O}(N^4)$  with a large prefactor, or as  $\mathcal{O}(N^5)$  (with the latter algorithm actually faster than the former for many molecules of interest).<sup>85</sup> Table II demonstrates timings on two systems from the parameterization dataset and two truncated proteinligand systems based on protein databank (PDB)<sup>100</sup> entry 3ACX. 101 SAPT0-D4/aDZ shows about a 9% to 19% reduction in compute time versus SAPT0/aDZ for dimer systems of 22 to 157 atoms. Due to the reduced scaling, the savings will clearly only increase as the system sizes increase. Furthermore, SAPT0-D4/aDZ demonstrates 76% and 95% reductions in compute time versus SAPT(DFT)/aDZ and SAPT(DFT)/aTZ, respectively, on the 22 atom system, and these differences grow to 78% and 97% on the 42 atom system.

These massive reductions in compute time of SAPT0-D4 compared to SAPT(DFT) make an argument for preferring the more inexpensive model, especially after considering the error statistics. In the case of SAPT0-D4/aDZ versus SAPT(DFT)/aDZ, the more inexpensive model, especially after considering the error statistics.

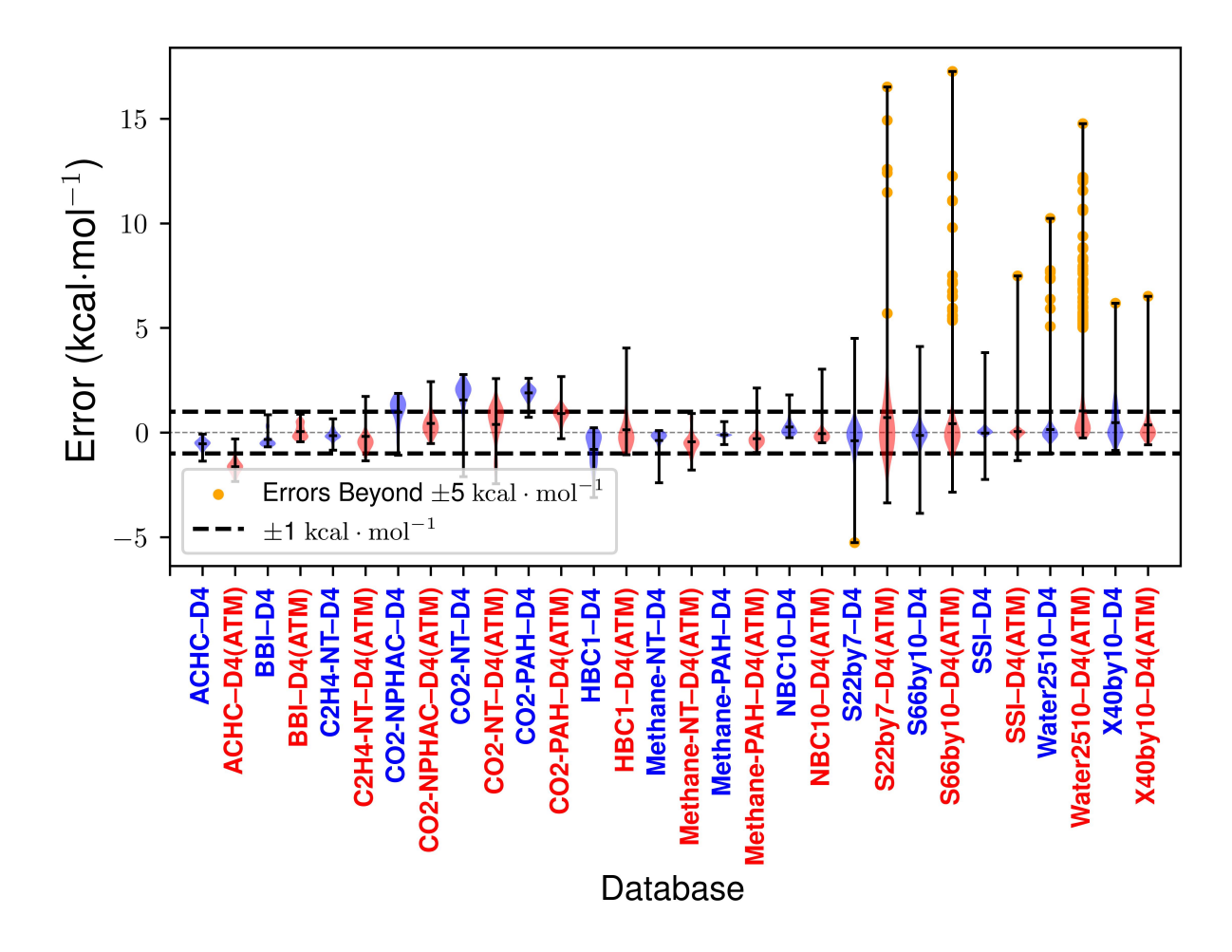


FIG. 3. Errors [versus CCSD(T)/CBS] for optimized SAPT0-D4/aDZ using only two-body terms, compared to the same level of theory when ATM is enabled [denoted SAPT0-D4(ATM)] using the original recommended HF-D4 parameters <sup>40</sup> shown in Table I. Violin plots are shown for each database within the overall dataset of 8299 dimers. The original HF-D4 damping parameters, fit to a smaller dataset, fail to sufficiently damp very close contact interactions featured in some of the datasets, drastically overbinding and causing large maximum negative errors.

sive model at roughly a quarter of the cost actually exhibits superior MAE and RMSE statistics, by 0.23 and 0.22 kcal mol<sup>-1</sup>, respectively. SAPT(DFT)/aTZ does remain the most accurate in Figure 4. On average, SAPT(DFT)/aTZ is about 0.14 kcal mol<sup>-1</sup> more accurate than SAPT0-D4/aDZ. This places SAPT0-D4/aDZ as a model between SAPT(DFT)/aDZ and SAPT(DFT)/aTZ in accuracy, while it is about 17 and 26 times faster than SAPT(DFT)/aTZ for systems as small as 22 and 42 atoms respectively. This factor will only grow for larger systems.

Thus, SAPT0-D4/aDZ appears to be a very promising model for accurate yet relatively rapid computation of interaction energies. We do note, however, that the good performance of SAPT0-based models for interaction energies benefits substantially from error cancellation between the individual energy components, <sup>79</sup> and that we expect SAPT(DFT) to provide more accurate component energies. <sup>85</sup>

# D. Analysis of charged systems

Lastly, due to -D4 having charge-scaled  $C_6$ 's, it should theoretically perform better on charged systems than its -D3 predecessor. Therefore, SAPT0-D3 and SAPT0-D4 error distributions are compared directly in Figure 5 for a subset of charged systems from the total dataset. Ultimately, most of the MAE's are similar, around 0.6 kcal mol<sup>-1</sup>, except for SAPT(DFT) and regular SAPT0. Surprisingly, SAPT(DFT)/aDZ struggles the most with handling these charged systems on average, even though the MaxAE is smaller. Also surprisingly, SAPT0/aDZ and SAPT(DFT)/aTZ perform very similarly, with nearly the same MAE and RMSE, even though SAPT(DFT)/aTZ does have a better MaxAE.

Based on the percentiles, SAPT0-D4/jDZ exhibits a tighter error distribution than SAPT0-D3/jDZ. Similarly, SAPT0-D4/aDZ's distribution is tighter than the

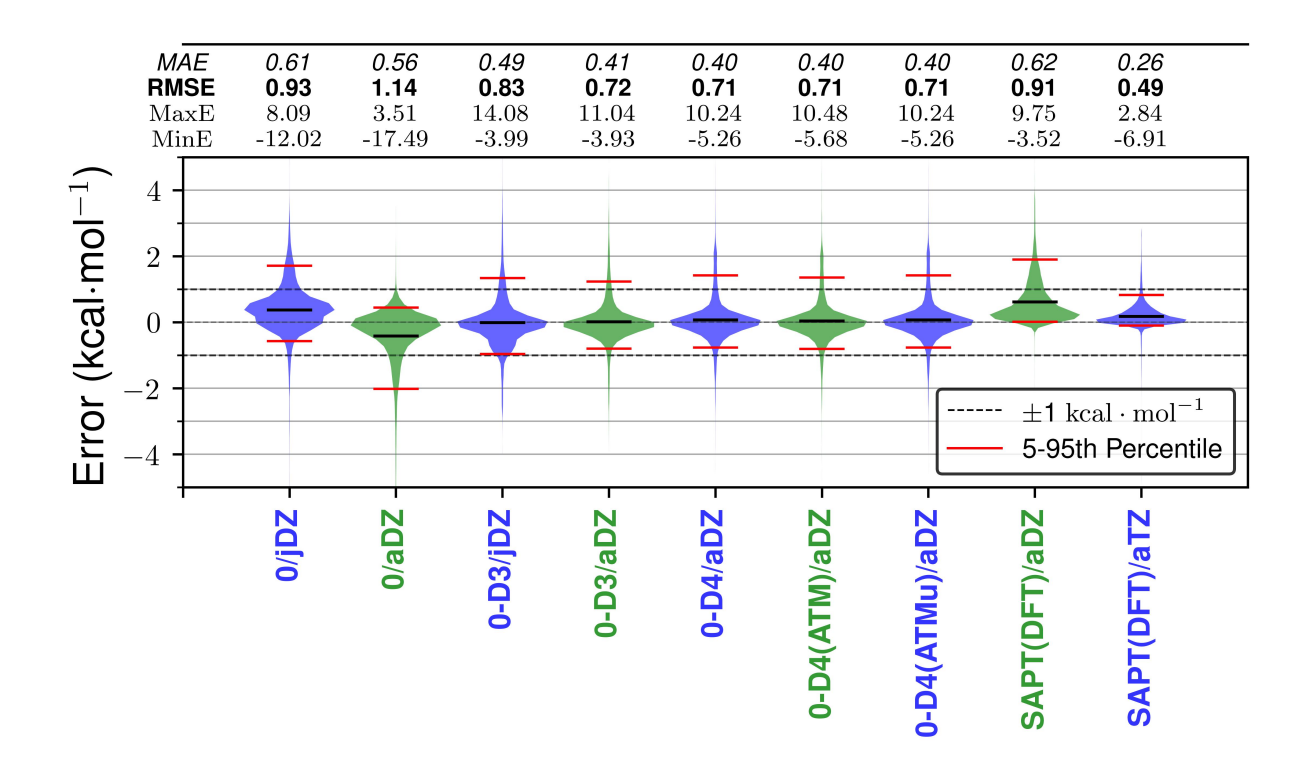


FIG. 4. Errors [vs. CCSD(T)/CBS] for SAPT0, SAPT0-D3, SAPT0-D4, SAPT0-D4(ATM), and SAPT(DFT) for the 8299-dimer dataset are compared with different damping function parameters and two damping functions. (ATM) denotes inclusion of ATM terms, with the 3B-CHG damping function. -D4(ATM) refers to sharing the  $a_1$  and  $a_2$  damping function parameters for 2B and 3B terms, while ATMu denotes separate damping parameters for 2B and 3B terms. "0" stands for SAPT0.

TABLE II. Timings (s) on (A) fragments of alanine and glycine protein-backbone interactions (22 atoms), (B) a partial carbon-nanotube interacting with ethylene (42 atoms), (C) 3ACX truncated system (83 atoms), and (D) 3ACX truncated system (157 atoms). These timings are acquired using 18 cores on an Intel(R) Core(TM) i9-10980XE with a modified Psi4 version 1.9. SAPT(DFT)/aTZ is not computed on C because it required more memory than available on the machine at 256 GB. Notably, the large memory demand comes from the SAPT(DFT) dispersion.

Sys.	Atoms	SAPT0-D4	SAPT0	SAPT(DFT)	SAPT(DFT)
		(aDZ)	(aDZ)	(aDZ)	(aTZ)
A	22	37	41	153	699
В	42	267	292	1215	7654
$^{\rm C}$	83	1485	1724	7145	-
D	157	28549	35377	-	-

SAPT0-D3/aDZ distribution, but the difference is more minor. Compared to SAPT0-D3/aDZ, SAPT0-D4/aDZ reduces the RMSE by 0.05 kcal mol<sup>-1</sup> and the MaxAE by 2.13 kcal mol<sup>-1</sup> at the cost of 0.1 kcal mol<sup>-1</sup> MAE increase. Hence, the new -D4 improvement does not seem as impactful as one might hope for charged systems.

Surprisingly, nearly all the SAPT(DFT) results for aDZ and aTZ are consistently overbinding for these

charged systems, even though the MaxAE's are among the lowest of the models compared. The RMSE of SAPT0-D4/aDZ is nearly 0.26 kcal mol<sup>-1</sup> lower than that of the much more expensive SAPT(DFT)/aTZ method for the charged systems. Overall, SAPT0-D3 is the best if MAE is the most important metric, but SAPT0-D4/aDZ and SAPT(DFT)/aTZ are better if MaxAE is more valued.

#### E. Component Analysis

A key reason to perform a SAPT computation is to obtain the energy components, which can provide more physical insight into an intermolecular interaction.<sup>4</sup> Hence, we have also examined the errors in the SAPT0-D3/D4 energy components, compared to highlevel SAPT SAPT2+3(CCD) $\delta$ MP2 data from Ref. 79. SAPT component errors vs SAPT2+3(CCD) $\delta$ MP2/augcc-pVTZ reference values for a large set of 4558 dimers are presented in Figure 6. For comparison purposes, the Figure includes results for a handful of wavefunction-based SAPT methods, as well as SAPT(DFT) (based on the PBE0 functional).

For both SAPT0 and SAPT(DFT), the electrostatics, exchange, and induction terms do not significantly improve from going from aDZ to aTZ, suggesting that these

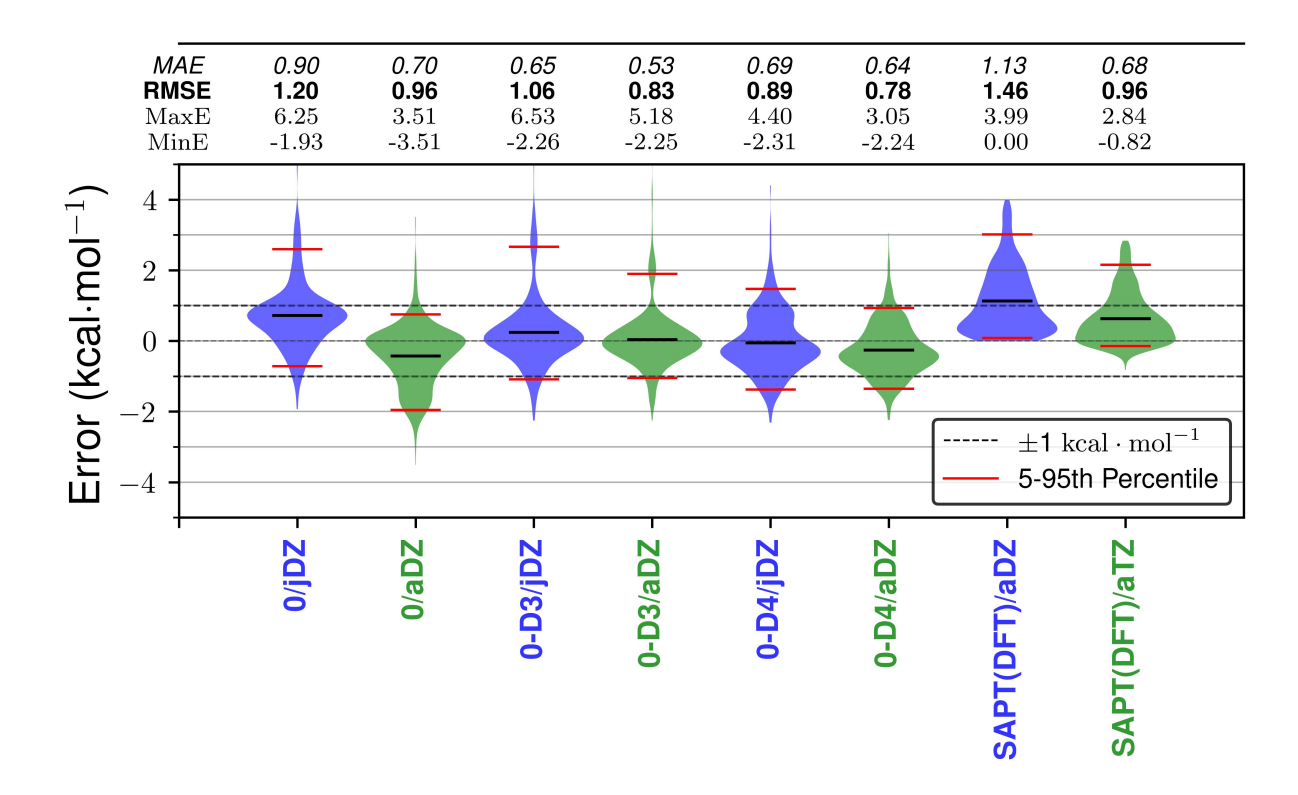


FIG. 5. Errors [versus CCSD(T)/CBS] for SAPT0-D3, SAPT0-D4, SAPT0-D4(ATM), and SAPT0 are compared for charged systems totaling 777 dimers in the dataset. The charged-scaled polarizabilities would be expected to provide an improvement in -D4 versus -D3. SAPT0 is labeled as "0" for simplifying the x-labels.

terms are converged much faster with respect to basis set size compared to the dispersion. This is consistent with the general findings of Refs. 79 and 102. Wavefunction-based SAPT including intramolecular correlation (i.e., SAPT2 and higher) show more variation in the component error statistics with respect to basis set, but are also not very sensitive to basis for these three energy components.

In general, the dispersion components show more variation with respect to basis, which is not surprising, because it is heavily dependent on electron correlation effects. An exception is the small basis set variations in the SAPT0-D3/D4 dispersion error statistics. The reason there is any basis set variation in these terms at all is that we used the damping parameters optimized for each basis set separately. As previously discussed, these damping parameters are not very different, and so very similar error statistics are the result. We note that the SAPT(DFT) dispersion component is much more sensitive to basis than the other SAPT(DFT) energy components, and the basis set improvement from aDZ to aTZ reduces the MAE by more than half.

Figure 6 further suggests that the accuracy of SAPT0's total energies does rely on favorable error cancellation.<sup>79</sup> The SAPT0 errors in exchange are on average negative (and very slightly negative for electrostatics and induction), leading to a need for a positive dispersion error

to acquire better total interaction energies. The SAPTO dispersion errors in the aug-cc-pVDZ basis do tend to be positive, by about the right amount to effectively cancel out the average negative exchange errors. In the aug-cc-pVTZ basis, this error cancellation between components is less effective, because the errors in electrostatics, exchange, and induction are not much changed, but now the errors in dispersion are improved and become less positive on average.

As shown in Figure 6, replacement of SAPT0 dispersion with -D3 or -D4 models and fitting the parameters to CCSD(T)/CBS energies promotes larger positive dispersion errors to more effectively cancel the negative errors of the other components, and thus yield smaller errors in total interaction energies. It is disappointing to see that both the MAE and also the RMSE of the SAPT0-D3/D4 dispersion energies are larger than those of the base SAPT0 model itself; apparently, in order to obtain good error cancellation in the total interaction energy, this is necessary to offset the significant negative errors (and significant spread in errors) in the SAPT0 exchange values.

Figure 7 provides a similar analysis for a subset of 358 dimers for which SAPT2+3(CCD) $\delta$ MP2/aug-cc-pVQZ components are available as reference values. The error statistics show very little change for non-dispersion terms as one progresses from aTZ to aQZ; about the

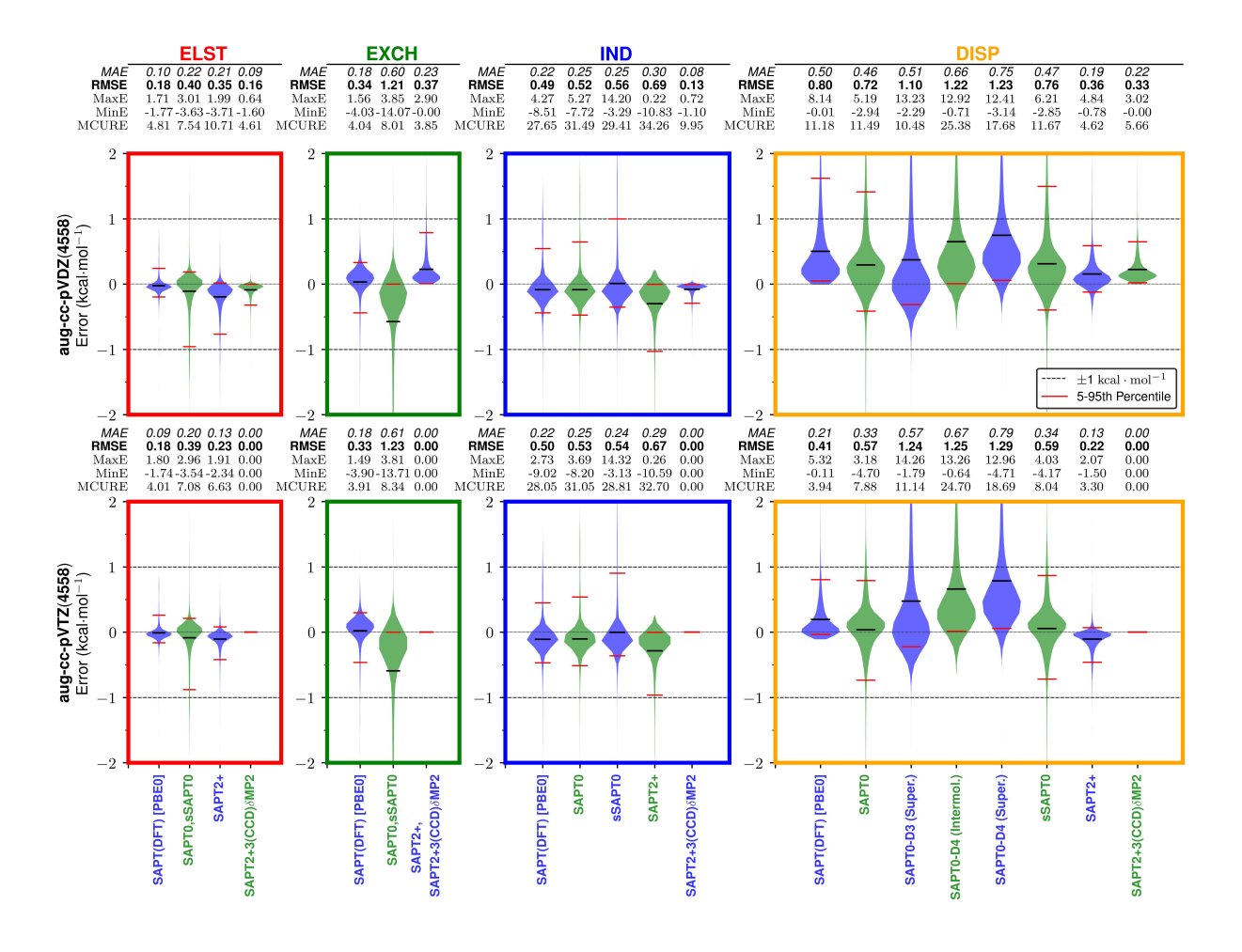


FIG. 6. SAPT component errors [versus SAPT2+3(CCD) $\delta$ MP2/aug-cc-pVTZ] for SAPT0-D3, SAPT0-D4 and SAPT(DFT) with aug-cc-pVDZ and aug-cc-pVTZ on a 4558 dimer dataset. Some levels of SAPT share the same components, so these terms are placed on the same line with a comma separating method names. Note that SAPT0 and SAPT0-D3/D4 are identical for electrostatics, exchange-repulsion, and induction terms.

only noticeable difference is a correction of some small positive exchange errors for SAPT2+ and related methods. For the dispersion term, again the basis set improvement leads to improved error statistics for SAPT0 and SAPT(DFT), although the improvements are more modest than they were for the change from aDZ to aTZ. These findings are in agreement with a previous study on the XSAPT method in which the non-dispersion terms were shown to converge faster with respect to basis set than the dispersion term. <sup>102</sup> In agreement with the analysis of Figure 6, there are significant errors in the SAPT0-D3/D4 dispersion components compared to high-level SAPT, apparently necessary to offset significant negative errors in SAPT0 exchange.

#### IV. CONCLUSIONS

The present work extends an earlier exploration of using Grimme's semi-empirical -D3 dispersion correction 14

to replace the dispersion term in Hartree–Fock based symmetry-adapted perturbation theory (SAPT0).<sup>50</sup> Whereas that study optimized damping parameters specifically for the truncated jun-cc-pVDZ basis set, this work examines a wider range of seven basis sets. Optimizing damping function parameters vs CCSD(T)/CBS estimates of the interaction energies of 8299 small van der Waals dimers, we find that SAPT0-D3/aug-cc-pVDZ reduces the mean absolute error on the test set by 0.08 kcal mol<sup>-1</sup> vs SAPT0-D3/jun-cc-pVDZ, and that optimal damping function parameters are quite similar across the basis sets considered.

We also considered an analogous model, SAPT0-D4, based on Grimme's newer -D4 correction. 40-42 Both SAPT0-D3 and SAPT0-D4 show significant improvements over conventional SAPT0, while also substantially reducing computational cost. Like SAPT0-D3, the damping function parameters in SAPT0-D4 are quite transferable across basis sets. The accuracy of SAPT0-D4 is very similar to that of SAPT0-D3, regardless

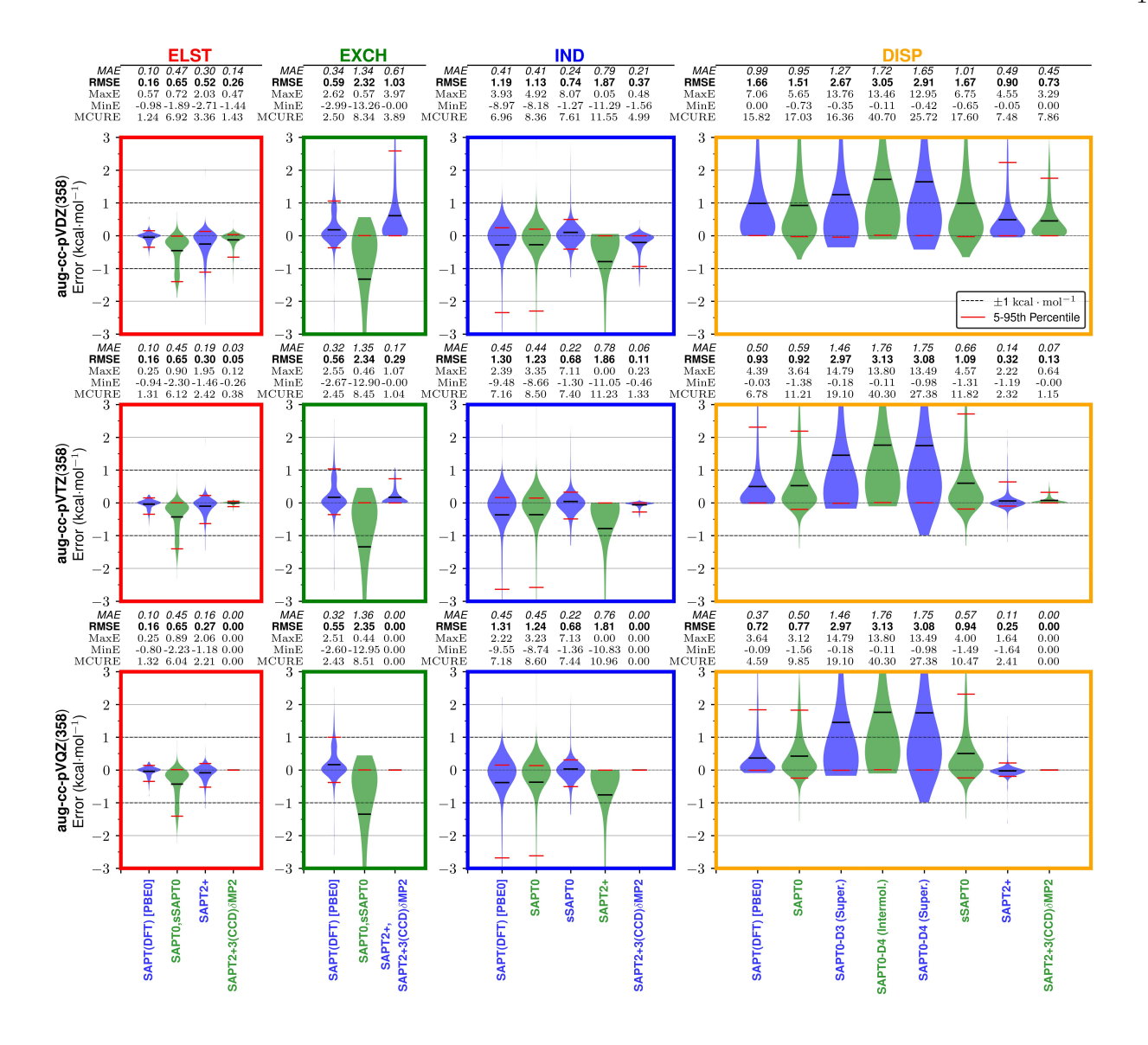


FIG. 7. SAPT component errors [versus SAPT2+3(CCD) $\delta$ MP2/aug-cc-pVQZ] for SAPT0-D3, SAPT0-D4 and SAPT(DFT) on a 358 dimer subset that has aug-cc-pVQZ results in addition to aug-cc-pVDZ and aug-cc-pVTZ. Some levels of SAPT share the same components, so these terms are placed on the same line with a comma separating method names. Note that SAPT0 and SAPT0-D3/D4 are identical for electrostatics, exchange-repulsion, and induction terms.

of basis set. The error distribution in total interaction energies is somewhat tighter for SAPT0-D4/aug-cc-pVDZ than SAPT0-D3/aug-cc-pVDZ for charged systems, where SAPT0-D4 might be expected to show more of an improvement, but the mean absolute error is not improved. Regardless, we recommend SAPT0-D4 over SAPT0-D3 because of its slightly lower maximum errors over the dataset.

SAPT0-D3 and SAPT0-D4 both use only two-body dispersion terms. None of the attempts to include three-body dispersion through damped Axilrod-Teller-Muto (ATM) terms provided any benefit for this test set, possibly because the systems included here are too small to benefit from ATM. <sup>32,99</sup>

Finally, SAPT0-D4 is actually more accurate on average for total interaction energies than the much more sophisticated SAPT(DFT) approach, at least in the augce-pVDZ basis (although not in the aug-cc-pVTZ basis). This is quite surprising, as the computational cost of SAPT0-D4 is much lower, as demonstrated for a few test systems (SAPT0-D4 offers a 4.8X speedup for one 83-atom test case). However, the individual energy components from SAPT0-D4 are not as accurate as those in SAPT(DFT). Optimization of -D3/-D4 damping parameters to minimize errors in total interaction energies vs CCSD(T)/CBS benchmarks causes the dispersion energy errors to become more positive than they are for SAPT0, and the RMSEs also become larger. This is ap-

parently necessary to compensate for significant negative errors (with significant RMSEs) in the SAPT0 exchange component. Thus, the more accurate total interaction energies in SAPT0-D3/D4 vs SAPT0 come at the cost of larger errors in the dispersion energies. If the accuracy of total interaction energies is of prime interest, and components are wanted only for a qualitative or semi-quantitative analysis, then SAPT0-D3/D4 seem to be a helpful improvement over SAPT0, applicable to larger systems. On the other hand, if accurate energy components are needed, then SAPT(DFT) or a higher-order wavefunction-based SAPT approach remains preferable, despite the larger computational cost.

# SUPPLEMENTARY MATERIAL

See the supplementary material for additional plots of SAPT0-D3 and SAPT0-D4 accuracy when optimizing parameters for a specific basis set versus using parameters for the aug-cc-pVDZ basis set. Additionally, Cartesian coordinates are provided for all timings tests, and a pandas dataframe for accessing all geometries and energies for the 8299 dimer dataset.

#### **ACKNOWLEDGMENTS**

The authors would like to thank Dr. Lori Burns for assistance in testing -D4 code, and Dr. Jeff Schriber for helping formulate research objectives and sharing code to accelerate the beginning of the project.

Austin M. Wallace acknowledges support from the U.S. National Science Foundation Graduate Research Fellowship, Grant No. DGE-2039655. Additional financial support was provided by NSF Grant No. CHE-1955940. This research was supported, in part, by research cyberinfrastructure resources and services provided by the Partnership for an Advanced Computing Environment (PACE) at the Georgia Institute of Technology, and by the Georgia Tech Hive Cluster, funded by the NSF through Grant No. MRI-1828187.

#### **DATA AVAILABILITY**

The data that support the findings of this study are available within this article and its supplementary material. The code to optimize parameters, recreate figures presented in this work, and access the dataset is publicly available on GitHub (see Ref. 94).

- <sup>1</sup>B. Jeziorski, R. Moszynski, and K. Szalewicz, Chem. Rev. **94**, 1887 (1994).
- <sup>2</sup>K. Szalewicz, Wiley Interdiscip. Rev. Comput. Mol. Sci. 2, 254 (2012).
- <sup>3</sup>E. G. Hohenstein and C. D. Sherrill, Wiley Interdiscip. Rev. Comput. Mol. Sci. 2, 304 (2012).
- <sup>4</sup>C. D. Sherrill, Acc. Chem. Res. **46**, 1020 (2013).

- <sup>5</sup>K. Patkowski, Wiley Interdiscip. Rev. Comput. Mol. Sci. 10, e1452 (2020).
- <sup>6</sup>E. G. Hohenstein, R. M. Parrish, C. D. Sherrill, J. M. Turney, and H. F. Schaefer, J. Chem. Phys. **135**, 174107 (2011).
- <sup>7</sup>R. M. Parrish, T. M. Parker, and C. D. Sherrill, J. Chem. Theor. Comput. **10**, 4417 (2014).
- <sup>8</sup>J. Hepburn, G. Scoles, and R. Penco, Chemical Physics Letters 36, 451 (1975).
- <sup>9</sup>R. Ahlrichs, R. Penco, and G. Scoles, Chemical Physics 19, 119 (1977).
- <sup>10</sup>C. Douketis, G. Scholes, S. Marchetti, M. Zen, and A. J. Thakkar, J. Chem. Phys. **76**, 3057 (1982).
- <sup>11</sup>Q. Wu and W. Yang, J. Chem. Phys. **116**, 515 (2002).
- <sup>12</sup>S. Grimme, J. Comput. Chem. **25**, 1463 (2004).
- <sup>13</sup>S. Grimme, J. Comput. Chem. **27**, 1787 (2006).
- <sup>14</sup>S. Grimme, J. Antony, S. Ehrlich, and H. Krieg, J. Chem. Phys. 132, 154104 (2010).
- <sup>15</sup>S. Grimme, S. Ehrlich, and L. Goerigk, J. Comput. Chem. **32**, 1456 (2011).
- <sup>16</sup>R. Sure and S. Grimme, Journal of computational chemistry 34, 1672 (2013).
- <sup>17</sup>S. Grimme, J. G. Brandenburg, C. Bannwarth, and A. Hansen, J. Chem. Phys. **143**, 054107 (2015).
- <sup>18</sup>A. J. Misquitta and K. Szalewicz, Chem. Phys. Lett. **357**, 301 (2002).
- <sup>19</sup>H. L. Williams and C. F. Chabalowski, J. Phys. Chem. A **105**, 646 (2001).
- <sup>20</sup>R. Podeszwa, K. Pernal, K. Patkowski, and K. Szalewicz, The Journal of Physical Chemistry Letters 1, 550 (2010).
- <sup>21</sup>A. J. Misquitta, R. Podeszwa, B. Jeziorski, and K. Szalewicz, The Journal of chemical physics 123, 214103 (2005).
- <sup>22</sup>A. Hesselmann, G. Jansen, and M. Schütz, J. Chem. Phys. **122**, 014103 (2005).
- <sup>23</sup> A. Hesselmann, The Journal of Physical Chemistry A 115, 11321 (2011).
- <sup>24</sup>K. U. Lao and J. M. Herbert, J. Phys. Chem. Lett. 3, 3241 (2012).
- <sup>25</sup>T. Takatani, E. G. Hohenstein, M. Malagoli, M. S. Marshall, and C. D. Sherrill, J. Chem. Phys. **132**, 144104 (2010).
- <sup>26</sup> J. Rezác, K. E. Riley, and P. Hobza, J. Chem. Theory Comput. 7, 2427 (2011).
- <sup>27</sup>K. U. Lao and J. M. Herbert, J. Chem. Phys. **139**, 034107 (2013).
- <sup>28</sup>K. U. Lao and J. M. Herbert, J. Chem. Phys. **140**, 119901 (2014).
- <sup>29</sup>K. U. Lao and J. M. Herbert, The Journal of Physical Chemistry A 119, 235 (2015).
- <sup>30</sup>K. Tang and J. Toennies, J. Chem. Phys. **66**, 1496 (1977).
- <sup>31</sup>K. Tang and J. P. Toennies, J. Chem. Phys. **80**, 3726 (1984).
- <sup>32</sup>K. Carter-Fenk, K. U. Lao, K.-Y. Liu, and J. M. Herbert, The journal of physical chemistry letters 10, 2706 (2019).
- <sup>33</sup>A. Tkatchenko, R. A. DiStasio, R. Car, and M. Scheffler, Phys. Rev. Lett. **108**, 236402 (2012).
- <sup>34</sup> A. Ambrosetti, A. M. Reilly, R. A. DiStasio, and A. Tkatchenko, J. Chem. Phys. **140**, 18A508 (2014).
- <sup>35</sup>B. Axilrod and E. Teller, J. Chem. Phys. **11**, 299 (1943).
- <sup>36</sup>Y. Muto, J. Phys. Math. Soc. Jpn **17**, 629 (1943).
- <sup>37</sup>R. Sedlak, T. Janowski, M. Pitoňak, J. Řezáč, P. Pulay, and P. Hobza, J. Chem. Theory Comput. 9, 3364 (2013).
- <sup>38</sup> J. Calbo, E. Ortí, J. C. Sancho-García, and J. Aragó, J. Chem. Theory Comput. **11**, 932 (2015).
- <sup>39</sup>R. Sedlak and J. Řezáč, Journal of Chemical Theory and Computation 13, 1638 (2017).
- <sup>40</sup>E. Caldeweyher, C. Bannwarth, and S. Grimme, J. Chem. Phys. 147, 034112 (2017).
- <sup>41</sup>E. Caldeweyher, S. Ehlert, A. Hansen, H. Neugebauer, S. Spicher, C. Bannwarth, and S. Grimme, J. Chem. Phys. 150, 154122 (2019).
- <sup>42</sup>E. Caldeweyher, J.-M. Mewes, S. Ehlert, and S. Grimme, Phys. Chem. Chem. Phys. **22**, 8499 (2020).

- <sup>43</sup> J. Řezáč, K. E. Riley, and P. Hobza, J. Chem. Theory Comput. 7, 3466 (2011).
- <sup>44</sup>S. Ehlert, S. Grimme, J. Antony, S. Ehrlich, and H. Krieg, DFTD3: dispersion correction for DFT, Hartree-Fock, and semiempirical quantum chemical methods. For the current version, see https://github.com/dftd3/simple-dftd3 (accessed July 2024). For the originating project, see https://www.chemie. uni-bonn.de/grimme/de/software/dft-d3.
- <sup>45</sup>S. Ehlert, S. Ehrlich, and E. Caldeweyher, DFTD4: generally applicable atomic-charge dependent London dispersion correction. For the current version, see https://github.com/dftd4/dftd4 (accessed July 2024).
- <sup>46</sup>K. Raghavachari, G. W. Trucks, J. A. Pople, and M. Head-Gordon, Chem. Phys. Lett. **157**, 479 (1989).
- <sup>47</sup>E. R. Johnson and A. D. Becke, J. Chem. Phys. **124**, 174104 (2006).
- <sup>48</sup>J.-D. Chai and M. Head-Gordon, Phys. Chem. Chem. Phys. **10**, 6615 (2008).
- <sup>49</sup>D. G. Smith, L. A. Burns, K. Patkowski, and C. D. Sherrill, J. Phys. Chem. Lett. 7, 2197 (2016).
- <sup>50</sup>J. B. Schriber, D. A. Sirianni, D. G. Smith, L. A. Burns, D. Sitkoff, D. L. Cheney, and C. D. Sherrill, J. Chem. Phys. 154, 234107 (2021).
- <sup>51</sup>T. H. Dunning, J. Chem. Phys. **90**, 1007 (1989).
- <sup>52</sup>E. Papajak and D. G. Truhlar, J. Chem. Theory Comput. 7, 10 (2011).
- <sup>53</sup>È. Papajak, J. Zheng, X. Xu, H. R. Leverentz, and D. G. Truhlar, J. Chem. Theory Comput. 7, 3027 (2011).
- <sup>54</sup>T. M. Parker, L. A. Burns, R. M. Parrish, A. G. Ryno, and C. D. Sherrill, J. Chem. Phys. **140**, 094106 (2014).
- <sup>55</sup>C. Villot and K. U. Lao, The Journal of Chemical Physics **160**, 184103 (2024).
- <sup>56</sup>M. S. Marshall, L. A. Burns, and C. D. Sherrill, J. Chem. Phys. 135, 194102 (2011).
- <sup>57</sup>K. S. Thanthiriwatte, E. G. Hohenstein, L. A. Burns, and C. D. Sherrill, J. Chem. Theory Comput. 7, 88 (2011).
- <sup>58</sup>I. G. Kaplan, Intermolecular interactions: physical picture, computational methods and model potentials. John Wiley & Sons, 2006.
- <sup>59</sup>D. C. Ghosh and N. Islam, Int. J. Quantum Chem. **110**, 1206 (2010).
- <sup>60</sup>G. Starkschall and R. G. Gordon, J. Chem. Phys. **56**, 2801 (1972).
- <sup>61</sup>A. J. Thakkar, H. Hettema, and P. E. Wormer, J. Chem. Phys. 97, 3252 (1992).
- <sup>62</sup>A. D. Becke and E. R. Johnson, J. Chem. Phys. **123**, 154101 (2005).
- <sup>63</sup>E. R. Johnson and A. D. Becke, J. Chem. Phys. **123**, 024101 (2005).
- <sup>64</sup>L. Goerigk, H. Kruse, and S. Grimme, ChemPhysChem 12, 3421 (2011).
- <sup>65</sup>B. Brauer, M. K. Kesharwani, S. Kozuch, and J. M. Martin, Phys. Chem. Chem. Phys. **18**, 20905 (2016).
- <sup>66</sup>L. Gráfová, M. Pitonak, J. Rezac, and P. Hobza, J. Chem. Theory Comput. 6, 2365 (2010).
- <sup>67</sup>D. E. Taylor et al., J. Chem. Phys. **145**, 124105 (2016).
- <sup>68</sup>T. M. Parker and C. D. Sherrill, J. Chem. Theory Comput. **11**, 4197 (2015).
- <sup>69</sup>D. G. Smith and K. Patkowski, J. Phys. Chem. C **119**, 4934 (2015).
- <sup>70</sup>L. A. Burns, Á. V. Mayagoitia, B. G. Sumpter, and C. D. Sherrill, J. Chem. Phys. **134**, 084107 (2011).
- <sup>71</sup>P. Jurečka, J. Šponer, J. Černỳ, and P. Hobza, Phys. Chem. Chem. Phys. **8**, 1985 (2006).
- <sup>72</sup> J. Rezac, K. E. Riley, and P. Hobza, J. Chem. Theory Comput. 8, 4285 (2012).

- <sup>73</sup>L. A. Burns, J. C. Faver, Z. Zheng, M. S. Marshall, D. G. Smith, K. Vanommeslaeghe, A. D. MacKerell Jr, K. M. Merz Jr, and C. D. Sherrill, J. Chem. Phys. **147**, 161727 (2017).
- <sup>74</sup>R. Bukowski, K. Szalewicz, G. C. Groenenboom, and A. Van der Avoird, Science 315, 1249 (2007).
- <sup>75</sup>R. Bukowski, K. Szalewicz, G. C. Groenenboom, and A. van der Avoird, J. Chem. Phys. **128**, 094313 (2008).
- <sup>76</sup>K. Patkowski, Annu. Rep. Comput. Chem. **13**, 3 (2017).
- <sup>77</sup>A. L. East and W. D. Allen, J. Chem. Phys. **99**, 4638 (1993).
- <sup>78</sup>A. G. Csaszar, W. D. Allen, and H. F. Schaefer III, J. Chem. Phys. **108**, 9751 (1998).
- <sup>79</sup>J. B. Schriber, D. L. Cheney, and C. D. Sherrill, ChemRxiv, https://doi.org/10.26434/chemrxiv-2023-ftt1v, 2023.
- <sup>80</sup>K. U. Lao, R. Schäffer, G. Jansen, and J. M. Herbert, J. Chem. Theor. Comput. **11**, 2473 (2015).
- <sup>81</sup>A. M. Wallace, hrcl\_jobs a python-based repository for running functions in a highly distributed parallel manner with mpi4py, 2023, https://github.com/awallace42/hrcl\_jobs.
- <sup>82</sup>D. G. Smith et al., J. Chem. Phys. **152**, 184108 (2020).
- <sup>83</sup>A. Heßelmann and G. Jansen, Chemical physics letters 362, 319 (2002).
- <sup>84</sup>G. Jansen, Wiley Interdisciplinary Reviews: Computational Molecular Science 4, 127 (2014).
- <sup>85</sup>Y. Xie, D. G. Smith, and C. D. Sherrill, J. Chem. Phys. **157**, 024801 (2022).
- <sup>86</sup>M. Grüning, O. Gritsenko, S. Van Gisbergen, and n. E. Baerends, J. Chem. Phys. 114, 652 (2001).
- <sup>87</sup>A. J. Misquitta and K. Szalewicz, Chemical physics letters 357, 301 (2002).
- <sup>88</sup>J. P. Perdew, K. Burke, and M. Ernzerhof, Physical review letters 77, 3865 (1996).
- <sup>89</sup>C. Adamo and V. Barone, The Journal of chemical physics 110, 6158 (1999).
- <sup>90</sup>P. Virtanen, R. Gommers, T. E. Oliphant, M. Haberland, T. Reddy, D. Cournapeau, E. Burovski, P. Peterson, W. Weckesser, J. Bright, S. J. van der Walt, M. Brett, J. Wilson, K. J. Millman, N. Mayorov, A. R. J. Nelson, E. Jones, R. Kern, E. Larson, C. J. Carey, İ. Polat, Y. Feng, E. W. Moore, J. VanderPlas, D. Laxalde, J. Perktold, R. Cimrman, I. Henriksen, E. A. Quintero, C. R. Harris, A. M. Archibald, A. H. Ribeiro, F. Pedregosa, P. van Mulbregt, and SciPy 1.0 Contributors, Nature Methods 17, 261 (2020).
- <sup>91</sup>M. J. Powell, Comput. J. **7**, 155 (1964).
- <sup>92</sup>V. S. Vassiliadis and R. Conejeros, *Powell method: Powell Method*, pages 2001–2003. Springer US, Boston, MA, 2001.
- <sup>93</sup>W. Jakob, J. Rhinelander, and D. Moldovan, pybind11 — seamless operability between c++11 and python, 2016, https://github.com/pybind/pybind11.
- <sup>94</sup>A. M. Wallace and C. D. Sherrill, d4\_dimers a python-based repository for optimizing d4 damping parameters and plotting results, 2023, https://github.com/awallace42/d4\_dimers.
- <sup>95</sup>H. Krekel, B. Oliveira, R. Pfannschmidt, F. Bruynooghe, B. Laugher, and F. Bruhin, pytest 7.2, 2004.
- <sup>96</sup>L. A. Burns, M. S. Marshall, and C. D. Sherrill, J. Chem. Phys. 141, 234111 (2014).
- <sup>97</sup>M. O. Sinnokrot, E. F. Valeev, and C. D. Sherrill, J. Am. Chem. Soc. **124**, 10887 (2002).
- <sup>98</sup>R. M. Parrish and C. D. Sherrill, J. Chem. Phys. **141**, 044115 (2014).
- <sup>99</sup>C. Villot, F. Ballesteros, D. Wang, and K. U. Lao, The Journal of Physical Chemistry A **126**, 4326 (2022).
- <sup>100</sup>H. M. Berman, J. Westbrook, Z. Feng, G. Gilliland, T. N. Bhat, H. Weissig, I. N. Shindyalov, and P. E. Bourne, Nucleic acids research 28, 235 (2000).
- <sup>101</sup>F.-Y. Lin, C.-I. Liu, Y.-L. Liu, Y. Zhang, K. Wang, W.-Y. Jeng, T.-P. Ko, R. Cao, A. H.-J. Wang, and E. Oldfield, Proceedings of the National Academy of Sciences 107, 21337 (2010).
- <sup>102</sup>M. Gray and J. M. Herbert, Journal of Chemical Theory and Computation 18, 2308 (2022).